JOURNAL OF APPLIED ELECTROCHEMISTRY **23** (1993) 167–172

Mass transfer at gas sparged spherical electrodes

G. H. SEDAHMED

Chemical Engineering Department, Faculty of Engineering, Alexandria University, Alexandria, Egypt

Received 27 January 1992; revised 29 June 1992

Rates of mass transfer were measured for the cathodic reduction of $K_3Fe(CN)_6$ in a large excess of sodium hydroxide at a single sphere cathode stirred by oxygen evolved at a horizontal disc anode placed below. The effect of the oxygen discharge rate and sphere diameter were studied at different ferricyanide concentrations. The rate of mass transfer was found to increase by an amount ranging from 66% to 450% over the natural convection value depending on the operating conditions. The data were correlated using hydrodynamic boundary layer theory and Kolmogoroff's theory of isotropic turbulence. The data were found to fit the equation:

$$Sh = 2 + 0.21Sc^{0.33}\,(ed_s^4/v^3)^{0.268}$$

where e is the rate of energy dissipation/unit mass of the liquid. Previous data on mass transfer at fixed beds of spheres stirred by counterelectrode oxygen bubbles were also correlated.

List of Symbols

a	cross section area of the cell (cm^3)
a_1–a_7	constants
A	electrode area (cm^2)
b	exponent of ε in Equation 2
$\bar{b}$	exponent of $(Re \cdot Fr)$ in Equation 3
c	concentration of $K_3Fe\,(CN)_6$ ($mol\,cm^{-3}$)
d_p	particle diameter (cm)
d_s	sphere diameter (cm)
D	diffusivity ($cm^2\,s^{-1}$)
E	input mechanical energy to the cell (J)
e	specific energy dissipation ($cm^2\,s^{-3}$)
F	Faraday's constant
g	acceleration due to gravity ($cm\,s^{-2}$)
h	height of the gas liquid dispersion in the cell (cm)
i_L	limiting current density ($A\,cm^{-2}$)
I_{O_2}	current consumed in oxygen discharge (A)
K	mass transfer coefficient ($cm\,s^{-1}$)
l	characteristic length (cm)
P	pressure ($g\,cm^{-2}$)
R	gas constant ($J\,mol^{-1}\,K^{-1}$)
T	temperature (K)
V_g	superficial gas velocity ($cm\,s^{-1}$)
z	number of electrons involved in the reaction
Ar	Archimedes number $\frac{gl^3}{v^2}\frac{\varepsilon}{1-\varepsilon}$
Ga	Galileo number (gl^3/v^2)
Sc	Schmidt number (D/v)
Sh	Sherwood number (Kl/D)
Re	Reynold number ($V_g l/v$)
Fr	Froude number (V_g^2/gl)

Greek symbols

α	constant in Equations 4 and 10
γ	Re exponent in Equations 4 and 10
ε	void fraction (gas holdup)
ε_l	liquid holdup
ρ	solution density ($g\,cm^{-3}$)
v	kinematic viscosity ($cm^2\,s^{-1}$)

1. Introduction

Gas stirring is gaining importance as a means of enhancing the rate of mass transfer in electrolytic cells [1–17] in view of its cost effectiveness compared to mechanical stirring [1,2]. The high efficiency of gas sparging in enhancing the rate of heat and mass transfer is attributed to the ability of gas bubbles to induce radial flow as well as axial flow [18,19]. The stirring gas may be introduced externally or the cell can be designed in such a way as to exploit the gas evolved at the counterelectrode [3–9]. The latter method has many advantages, the most important of which is the saving of external stirring power. Previous studies on mass transfer at gas sparged electrodes have dealt with geometries such as vertical [4,13,18] and horizontal cylinders [6], vertical [12,14] and horizontal screens [3,15], vertical plates [1,2,5,16,17] and fixed beds [7,11]. The object of the present work is to study the effect of gas sparging on the rate of mass transfer at a single sphere electrode. Apart from the academic importance of this geometry, spheres are encountered in electrochemical practice e.g. electroplating, electroforming, electrochemical machining, electropolishing and electroless plating.

The present work was carried out using anodically generated oxygen as the stirring gas. The use of anodically generated gas has the advantage over externally introduced gas that the bubble characteristics e.g. bubble size, coalescence tendency and gas holdup are well studied [20,21]. Also, with proper cell design more uniform bubble distribution can be obtained. The rate

0021-891X

of mass transfer at the gas sparged sphere was measured by determining the limiting current of the cathodic reduction of potassium ferricyanide in a large excess of sodium hydroxide.

2. Theory

Mass transfer data in gas sparged cells have been correlated in different ways by different authors. Ibl [22] and Sigrist *et al.* [17] correlated results in a manner similar to that used in natural convection and found that their data fitted the equation:

$$Sh = 0.19\,(Sc \cdot Ar)^{0.33} \qquad (1)$$

Cavatorta and Bohm [10], Cavatorta *et al.* [13] and Pivano *et al.* [12] correlated data using a modified version of Ibl's method, where the gas holdup (ε) was separated from Ar; the authors correlated their data for different electrode and sparger geometries by the equation:

$$Sh = a_1(Sc \cdot Ga)^{0.33}\,\varepsilon^{b} \qquad (2)$$

The constants a_1 and b in the above equation depend on electrode geometry. Both Equations 1 and 2 need *a priori* determination of the gas holdup which is not always easy, beside the fact that it may not be uniform in the cell. To obviate the need to determine the gas holdup, Sedahmed [8] and Sedahmed *et al.* [14] correlated their data in a manner similar to that used in heat transfer in bubble columns, namely:

$$J = a_2(Re \cdot Fr)^{\bar{b}} \qquad (3)$$

The constants a_2, $\bar{b}$ depend on the geometry of the transfer surface. The criticism which might be levelled against Equation 3 is that it shows that the characteristic length of the transfer surface has no effect on the rate of mass transfer, which is not always true especially for transfer surfaces of small characteristic length.

The following represents an attempt to correlate mass transfer data at gas sparged spheres using the hydrodynamic boundary layer theory according to which the rate of mass transfer at a sphere in a cross flow is given by [23]

$$Sh = 2 + \alpha\, Sc^{0.33}\, Re^{\gamma} \qquad (4)$$

The difficulty of applying the above equation to gas sparged spheres is that the slip velocity, V, required to calculate Re is not known. This difficulty can be overcome by invoking Kolomogroff's theory of isotropic turbulence, the use of which is justified in gas sparged systems by virtue of the tubulent nature of the flow [17,24]. Combination of the hydrodynamic boundary layer theory and the Kolmogoroff theory of isotropic turbulence has been used successfully to correlate liquid-solid mass and heat transfer data in mechanically stirred systems [25,26] and gas sparged fluidized beds [27,28]. Turbulent flow prevails in bubble columns in the bubbly flow regime as a result of the formation of turbulent eddies in the wake of the rising bubbles; these eddies break down into micro scale eddies which extend their action toward the container wall [24]. Buchholz [29] measured turbulence intensities in bubble columns and found that the turbulence intensity is uniform over the cross sectional area.

According to Kolmogoroff [30,31] large scale low frequency primary eddies are produced by turbulent flow. Although these eddies contain the bulk of the kinetic energy they contribute only slightly to viscous energy dissipation. Interaction of the large eddies with slow moving streams produces smaller eddies of higher frequency, which further disintegrate until, finally, they are dissipated into heat by viscous forces, Kolmogoroff argued that the smaller eddies are independent of the bulk motion and are isotropic. The properties of these eddies are a function of the rate of energy dissipation per unit mass (e) and the kinematic viscosity. Based on dimensional reasoning Kolmogoroff derived the following equations for the length scale ($\bar{l}$) and the velocity scale (v) of the isotropic eddies

$$\bar{l} = (\nu^3/e)^{1/4} \qquad (5)$$

$$v = (\nu e)^{1/4} \qquad (6)$$

Kolmogoroff then postulated that the root mean square of the velocity difference $\bar{v}$ between two points at a distance d was given by

$$\bar{v}/v = f\,(d/\bar{l}) \qquad (7)$$

Using dimensional analysis Kolmogoroff derived the following expression:

$$\bar{l} < d < L \qquad \bar{v} = (ed)^{1/3} \qquad (8)$$

where L is the scale of a primary eddy, assuming d is equal to sphere diameter d_s, that is

$$d = d_s \qquad (9)$$

Substituting Equations 8 and 9 in Equation 4

$$Sh = 2 + \alpha Sc^{0.33}\,(e d_s^4/\nu^3)^{\gamma} \qquad (10)$$

The coefficient α and the exponent γ will be determined using the present experimental data. The rate of energy dissipation per unit mass (e) can be calculated by considering the total mechanical energy input to the cell (E) which is the product of the gas pressure drop in the cell and the volumetric gas flow rate.

$$E = gQ\Delta P = gV_g a h \rho \varepsilon_l \qquad (11)$$

The energy dissipated per unit mass of liquid is given by

$$e = gV_g \qquad (12)$$

It may be relevant to the present work to quote equations obtained for liquid–solid mass transfer at suspended particles in bubble columns. Sanger and Deckwer [27] correlated their data for ion exchange beads of various diameter by the equation

$$Sh = 2 + 0.545 Sc^{0.33}\left(\frac{e d_p^4}{\nu^3}\right)^{0.264}$$

Sano *et al.* [28] measured the mass transfer coefficients of suspended benzoic acid and naphthol particles in a bubble column; they correlated their data

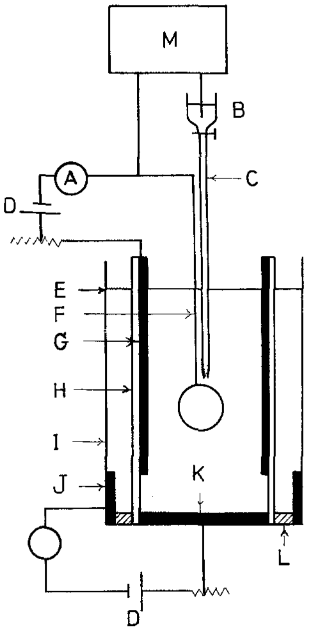

Fig. 1. Cell and electrical circuit. A, multirange ammeter; B, reference electrode; C, Luggin tube; D, 6 V d.c. power supply; E, electrolyte level; F, isolated current feeder; G, cylindrical Ni foil anode of cell 1; H, porous diaphragm; I, cylindrical plexiglass container; J, cathode of oxygen generating cell (cell 2); K, anode of oxygen generating cell (cell 2); L, wax seal; M, potentiometer.

with the equation

$$Sh = \phi\left[2 + 0.4Sc^{0.33}\left(\frac{ed_p^4}{v^3}\right)^{0.25}\right] \qquad (14)$$

3. Experimental technique

The apparatus (Fig. 1) consisted of two separate cells placed in the same container. Each cell was fed with current from a different d.c. source. One of the two cells served to generate oxygen (cell 2) which stirred the solution at the cathode of the other cell (cell 1) where ferricyanide ion was reduced from alkaline solution. The container was made of plexiglass and had a volume of 2 dm^3 and a diameter of 12 cm, it was divided into two compartments by a tight cylindrical porous diaphragm of 6.8 cm diameter made of synthetic fabric and supported on a perforated plastic cylinder. The inner compartment contained the cell used to measure the limiting current (cell 1) and the anode of the oxygen generating cell. The outer compartment contained the cathode of the oxygen generating cell. The oxygen generating cell consisted of a horizontal nickel disc anode of 6.7 cm diameter located at the bottom of the inner compartment at a distance 5 cm from the cathode of cell 1 and isolated from its back by epoxy resin; the cathode of the oxygen generating cell was made of a cylindrical nickel foil of 4 cm height, placed in the outer compartment. The cell used for limiting current measurement (cell 1) consisted of a nickel plated sphere cathode welded to an isolated current feeder which also acted as a cathode holder. The cell anode was made of a cylindrical nickel foil of 6.7 cm diameter surrounding the sphere cathode which was located in the centre of the cell. Preliminary experiments on the effect of distance between the sphere and the oxygen generating electrode showed that, under the present conditions, distance has a negligible effect on the mass transfer coefficient.

The electrical circuit connected to each cell was composed of a multirange ammeter and a 6 V d.c. power supply with a voltage regulator. Mutual electrical interference between the two cells was found to be negligible and each cell behaved independently during electrolysis. Before each run the cathode was activated as mentioned elsewhere [32]. The rate of oxygen discharge was controlled by adjusting the current passing through the oxygen generating cell; the current density used in oxygen generation ranged from 0.0125 to 0.125 A cm^{-2}. The oxygen discharge rate (superficial velocity) was calculated from the equation [33]

$$V_g = I_{O_2}RT/4FPA \qquad (15)$$

The limiting current for the cathodic reduction of ferricyanide ion was obtained potentiostatically [34–37]. The method consisted in fixing the cathode potential at a value of 350 mV corresponding to the limiting current and recording the steady state current. The cathode potential was measured against a reference electrode by means of a potentiometer. The reference electrode consisted of a nickel wire placed in the cup of a Luggin tube filled with a solution identical to the cell solution [38,39]. The Luggin tube had a small diameter (0.25 cm) in order to minimize its interference with the flow pattern of the gas-liquid dispersion; the tip of the Luggin tube, which was placed at 0.5–1 mm from the cathode surface, was plugged with a cotton filament to avoid entry of gas bubbles into the Luggin tube. During electrolysis no bubbles adhered to the sphere surface.

Three different concentrations of potassium ferricyanide were used 0.025, 0.05 and 0.1 M; in all cases 2 N NaOH was used as a supporting electrolyte. AR grade chemicals and distilled water were used in preparing the solutions. The viscosity and density of the solution were determined by means of an Ostwald viscometer and density bottle respectively [40]. Diffusivity of ferricyanide ion was calculated from the formula of Eisenberg *et al.* [41]. Solution temperature was 22 ± 1 °C. Each run was repeated once or twice using a fresh solution. The mass transfer coefficient was calculated from the limiting current using the equation

$$i_L/zF = KC \qquad (16)$$

4. Results and discussions

Figure 2 shows that the mass transfer coefficient at a single sphere electrode can be related to the rate of energy dissipation/unit mass of solution by the equation

$$K = a_3e^{0.268} \qquad (17)$$

which implies that the mass transfer coefficient is related to the superficial gas velocity by the equation

$$K = a_4V_g^{0.268} \qquad (18)$$

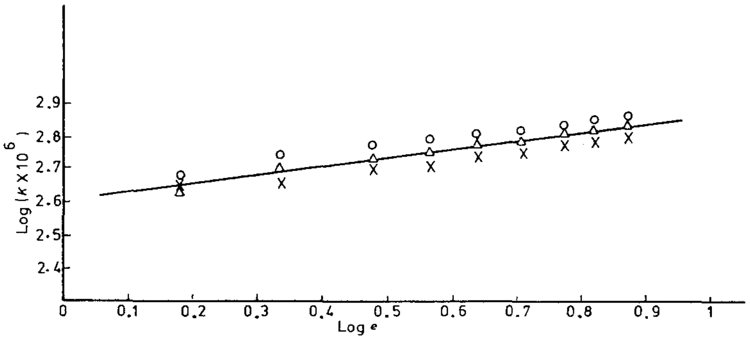

Fig. 2. Effect of the rate of energy dissipation per unit mass of the solution on the mass transfer coefficient at a single sphere electrode. Sphere diameter = 3.75 cm. Ferricyanide conc./M: (×) 0.025, (○) 0.05, and (△) 0.1

The V_g exponent 0.268 agrees with the previously reported values in heat and mass transfer in gas sparged systems which ranged from 0.19 to 0.37 depending on the geometry of the transfer surface and the range of superficial gas velocities. The exponent 0.268 also agrees with the value 0.25 predicated from heat and mass transfer models [16,28] obtained by combining the surface renewal theory with Kolmogoroff's theory of isotropic turbulence. The slight dependence of the data shown in Fig. 2 on ferricyanide concentration may be attributed to natural convection interference [34]. Recently, Zarraa *et al.* [42] studied the effect of nitrogen sparging on the rate of diffusion controlled dissolution of a single copper sphere in acidified chromate solution using a 10 cm diameter shallow bubble column fitted at its bottom with a multihole plastic distributor with each hole of 0.1 mm diameter. The authors used a superficial velocity range of 0.564–2.334 cm s^{-1} (the present range is 1.5×10^{-3}–7.5×10^{-3} cm s^{-1}) and a sphere diameter range of 0.48–3.5 cm. The mass transfer coefficient, which ranged from 0.001182 to 0.0167 cm s^{-1}, was related to the superficial nitrogen velocity by the equation

$$K = a_5 V_g^{0.565} \tag{19}$$

In the absence of an established exact mechanism which explains mass transfer in gas sparged systems it is difficult to account for the discrepancy between Equation 18 and Equation 19. However the results of the work of Whitney and Tobias [34] may be useful in this regard. These authors studied the effect of an electrolytically generated single bubble stream on the rate of mass transfer at a vertical planar micromosaic electrode placed downstream of the gas generating electrode. The authors came to the conclusion that bubbles rising within the mass transfer boundary layer enhance the rate of mass transfer through a surface renewal mechanism according to which

$$K = a_6 V_g^{0.5} \tag{20}$$

On the other hand bubbles rising outside the mass transfer boundary layer induce an upward flow which increases the velocity gradient at the electrode surface with a consequent increase in the mass transfer coefficient according to the equation.

$$K = a_7 V_g^{0.33} \tag{21}$$

In view of the finding of Whitney and Tobias the present V_g exponent, 0.268, of Equation 20 suggests that, under the present conditions, the rising bubble swarm moves outside the mass transfer boundary layer around the sphere. This is consistent with the fact that the rising oxygen bubbles are repelled away from the negatively charged sphere cathode because these bubbles carry a negative charge. Brandon and Kelsall [43] found that electrolytically generated oxygen bubbles from solutions having pH > 3 are negatively charged while bubbles generated from solution having pH < 2 are positively charged. The V_g exponent 0.565 of Equation 19, obtained by Zerraa *et al.*, suggests that the bubble swarm could penetrate the mass transfer boundary layer where the rate of mass transfer is enhanced by a surface renewal mechanism, as revealed by Whitney and Tobias. The close proximity between nitrogen bubbles and the sphere surface in the case of Zarraa's work may be attributed to the absence or weakness of repulsion between the rising nitrogen bubbles and the unpolarized copper spheres used by Zarraa *et al.*

Figure 3 shows that the mass transfer coefficient decreases with increasing sphere diameter and then remains almost constant with further increase in sphere diameter. This behaviour is consistent with the turbulent nature of the flow and agrees with the findings of other authors [5,6,8,44–47].

Figure 4 shows that the present mass transfer data

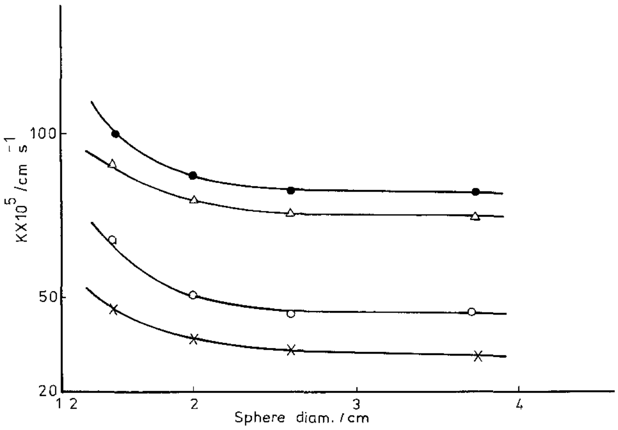

Fig. 3. Effect of sphere diameter on the mass transfer coefficient at a single sphere electrode. Ferricyanide conc. = 0.1 M. Oxygen discharge rate/cm^3 cm^{-2} s^{-1}: (×) 0.000826, (○) 0.0015, (△) 0.00526, and (●) 0.00751.

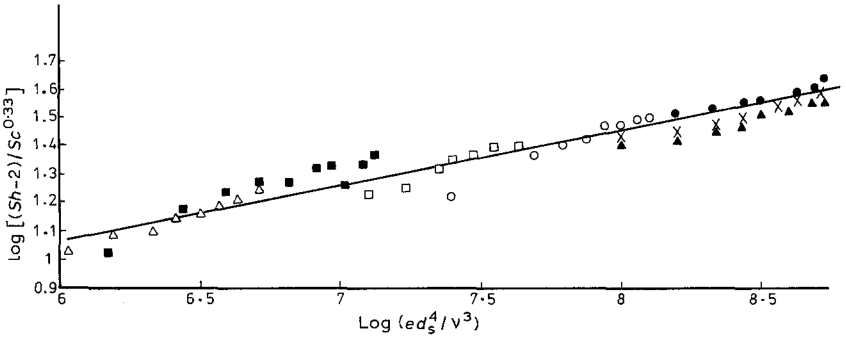

Fig. 4. Overall mass transfer correlation at gas sparged single sphere in terms of the specific energy dissipation. d/cm, ferricyanide conc./M: (×) 3.75, 0.1; (○) 2.6, 0.1; (△) 1.2, 0.1; (●) 3.75, 0.05; (▲) 3.75, 0.025; (□) 2, 0.1; and (■) 1.5, 0.1.

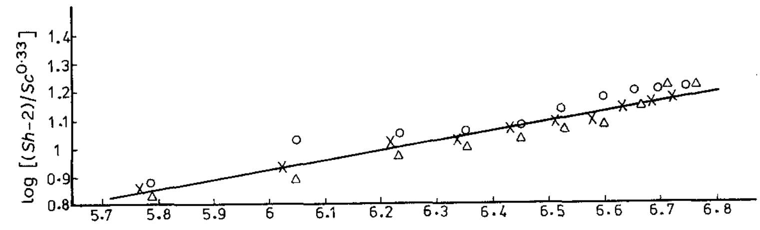

Fig. 5. Overall mass transfer correlation at a gas sparged fixed bed of spheres in terms of the specific energy dissipation. Sphere diameter = 1.2 cm. Ferricyanide conc./M: (×) 0.1, (○) 0.05, and (△) 0.025.

fit the equation

$$Sh = 2 + 0.21 Sc^{0.33} \left(\frac{e d_s^4}{\nu^3}\right)^{0.268} \qquad (22)$$

for the conditions $2860 < Sc < 2916 \times 10^6 > (ed^4/\nu^3) > 542 \times 10^6$ with an average deviation of ±15.7%. In calculating Sh, the sphere diameter was used as a characteristic length. In an earlier study using a technique similar to the present one Sedahmed [7] studied the rate of mass transfer at a cathode made of a single layer of closely packed spheres and stirred with oxygen bubbles evolved at a horizontal disc anode placed below the fixed bed. The rate of mass transfer was found to increase by a factor of 2–6.5 over the natural convection value without a voltage penalty as a result of the flow of oxygen bubbles through the fixed bed cathode. Figure 5 shows that the mass transfer data at a single layer of closely packed spheres stirred with counterelectrode oxygen bubbles fit the equation

$$Sh = 2 + 0.067 Sc^{0.33} \left(\frac{e d_s^4}{\nu^3}\right)^{0.33} \qquad (23)$$

for the conditions $2860 < Sc < 2916 \times 10^6$ $(ed^4/\nu^3) > 5.7 \times 10^6$ with an average deviation of ±7%.

A comparison between Equation 22 and Equation 23 shows that, for the same gas superficial velocity, the mass transfer coefficient is higher in the case of a single sphere by an amount ranging from 17% to 26%.

Since Equation 3 is used widely to correlate mass and heat transfer data in gas sparged systems [24,47] it would be useful, for the purpose of comparison with other heat and mass data in gas sparged systems, to correlate the present data in terms of Equation 3. Figure 6 shows that the present data for the conditions $0.25 \times 10^{-9} < Fr \cdot Re < 22.5 \times 10^{-9}$ fit the equation

$$J = 0.21\,(Re \cdot Fr)^{-0.245} \qquad (24)$$

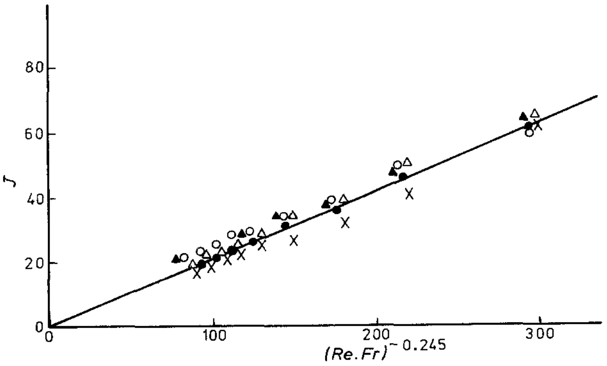

Fig. 6. Overall mass transfer correlation at a gas sparged single sphere using Equation 3. d/cm, ferricyanide conc./M: (×) 3.75, 0.025; (△) 3.75, 0.05; (●) 3.75, 0.025; (○) 2.6, 0.1; and (△) 2, 0.1.

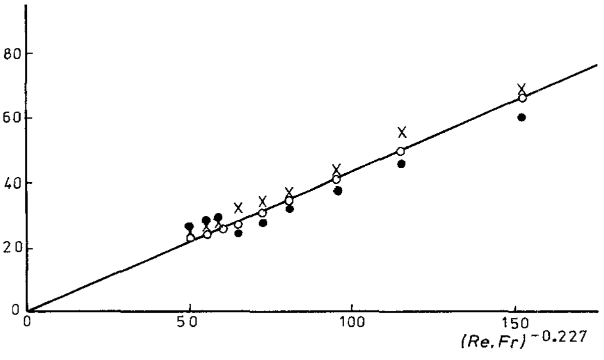

Fig. 7. Overall mass transfer correlation at a gas sparged fixed bed of spheres using Equation 3. Sphere diameter = 1.2 cm. Ferricyanide conc./M: (●) 0.025, (×) 0.05, and (○) 0.1.

with an average deviation of $\pm 8.9\%$. For a fixed bed of spheres, Fig. 7 shows that the data for the conditions $1.97 \times 10^{-9} < Re \cdot Fr < 31 \times 10^{-9}$ fit the equation

$$J = 0.43\,(Re \cdot Fr)^{-0.227} \tag{25}$$

with an average deviation of $\pm 8.5\%$.

5. Conclusions

(i) Gas sparging is an effective way of enhancing the rate of mass transfer at spherical electrodes. The degree of enhancement depends mainly on the superficial gas velocity, sphere diameter plays a secondary role under the present conditions.

(ii) Based on the hydrodynamic boundary layer theory and Kolomogroff's theory of isotropic turbulence the present data, as well as previous data on gas sparged fixed beds of spheres, were correlated in terms of the specific energy dissipation. This method does not suffer from the shortcomings of other correlating methods.

(iii) It is probable that the charge on the sparged bubbles plays an important role in determining the ability of the bubbles to enhance the rate of mass transfer at the polarized electrode. The degree of mass transfer enhancement increases if the bubbles carry a charge opposite to that of the polarized electrode at which mass transfer takes place and vice versa.

References

[1] N. Ibl, E. Adam, J. Venczel and E. Schalch, *Chem. Ing. Techn* **43** (1971) 202.
[2] A. S. Gendron and V. Ettel, *Can. J. Chem. Eng.* **53** (1975) 36.
[3] G. H. Sedahmed, *J. Appl. Electrochem.* **8** (1978) 339.
[4] *Idem*, *ibid.* **10** (1980) 351.
[5] G. H. Sedahmed and L. W. Shemilt, *ibid.* **11** (1981) 351.
[6] *Idem*, *Can. J. Chem. Eng.* **60** (1982) 767.
[7] G. H. Sedahmed, *ibid.* **64** (1986) 75.
[8] *Idem*, *J. Appl. Electrochem.* **14** (1984) 693.
[9] A. M. Ahmed and G. H. Sedahmed, *J. Electrochem. Soc.* **135** (1988) 2766.
[10] O. N. Cavatorta and U. Bohm, *J. Appl Electrochem.* **17** (1987) 340.
[11] L. Coppola, O. N. Cavatorta and U. Bohm, *ibid.* **19** (1989) 100.
[12] S. Piovano, O. N. Cavatorta and U. Bohm, *ibid.* **18** (1988) 128.
[13] O. N. Cavatorta, U. Bohm, A. M. Chiappori De Del Giorgio, *ibid.* **21** (1991) 40.
[14] G. H. Sedahmed, H. A. Farag, A. A. Zatout and F. A. Kathout, *ibid.* **16** (1986) 374.
[15] F. A. Katkout, A. A. Zatout, H. A. Farag and G. H. Sedahmed, *Can. J. Chem. Eng.* **66** (1988) 497.
[16] G. H. Sedahmed, *J. Appl. Electrochem.* **15** (1985) 777.
[17] L. Sigrist, O. Dossenbach and N. Ibl, *Int. J. Heat Mass Transfer* **22** (1979) 1393.
[18] W. Kast, *Chem. Ing. Techn* **35** (1963) 785.
[19] *Idem, Int. J. Heat Mass Transfer* **5** (1962) 329.
[20] L. J. Janssen and J. G. Hoogland, *Electrochem. Acta* **18** (1973) 543.
[21] G. Kreysa and M. Kuhn, *J. Appl. Electrochem.* **15** (1985) 517.
[22] N. Ibl, *Electrochim. Acta* **24** (1979) 1105.
[23] W. D. Deckwer and A. Schumpe, *Int. Chem. Engng.* **27** (1987) 405.
[24] W. D. Deckwer, *Chem. Eng. Sci.* **35** (1980) 1341.
[25] P. H. Calderbank and M. B. Moo-Young, *ibid.* **16** (1961) 39.
[26] D. M. Levins and J. R. Glastonburg, *ibid.* **27** (1972) 537.
[27] P. Sanger and W. D. Deckwer, *Chem. Eng. J.* **22** (1981) 179.
[28] Y. Sano, N. Yamagichi and T. Adachi, *J. Chem. Eng., Japan* **7** (1974) 255.
[29] R. Bucholz, Ph.D Thesis, University of Hanover (1979).
[30] A. N. Kolmogoroff, *C. R. Acad Sci. URSS* **31** (1941) 538.
[31] J. O. Hinze, 'Turbulence', McGraw-Hill, NY (1975).
[32] M. Eisenberg, C. W. Tobias and C. R. Wilke, *J. Electrochem. Soc.* **101** (1954) 306.
[33] T. R. Beck, *J. Electrochem. Soc.* **116** (1969) 1038.
[34] G. M. Whitney and C. W. Tobias, *AIChE. J* **34** (1988) 1981.
[35] L. J. J. Janssen and E. Barendrecht, *Electrochim. Acta* **24** (1979) 693.
[36] C. I. Elsner and S. L. Marchiano, *J. Appl. Electrochem.* **12** (1982) 735.
[37] F. N. Ngoya and J. Thonstad, *Electrochim. Acta* **30** (1985) 1959.
[38] J. R. Selman and C. W. Tobias, *Adv. in Chem. Eng.* **10** (1978) 211.
[39] M. G. Fouad and T. Gouda, *Electrochim. Acta* **9** (1964) 1071.
[40] A. Findlay and J. K. Kitchener, 'Practical Physical Chemistry', Longmans, London (1965).
[41] M. Eisenberg, C. W. Tobias and C. R. Wilke, *J. Electrochem. Soc.* **103** (1956) 413.
[42] M. A. Zarraa, Y. A. El-Tawil, H. A. Farag, M. Z. El-Abd and G. H. Sedahmed, *Chem. Eng. J.* **47** (1991) 187.
[43] N. P. Brandon and G. H. Kelsall, *J. Appl. Electrochem.* **15** (1985) 475.
[44] J. S. Gopal and M. M. Sharma, *Can. J. Chem. Eng.* **61** (1983) 517.
[45] V. Levich, 'Physicochemical Hydrodynamics', Prentice Hall, Englewood Cliffs, NJ (1962).
[46] D. A. Lewis, R. W. Feld, A. M. Xavier and D. Edwards, *Trans. Inst. Chem. Eng.* **60** (1982) 40.
[47] O. N. Cavatorta and U. Bohm, *Chem. Eng. Res. Des.* **66** (1988) 265.